AIAA CONFERENCE ON PHYSICS OF ENTRY INTO PLANETARY ATMOSPHERES

AUGUST 26-28, 1963, MASSACHUSETTS INSTITUTE OF TECHNOLOGY, KRESGE AUDITORIUM, CAMBRIDGE, MASSACHUSETTS

# NONEQUILIBRIUM HYPERSONIC BOUNDARY LAYER FLOW ALONG A SHARP FLAT PLATE WITH A STRONG INDUCED PRESSURE FIELD

by
GEORGE R. INGER
Aerospace Corp.
El Segundo, Calif.

No. 63-442

# NONEQUILIBRIUM HYPERSONIC BOUNDARY LAYER FLOW ALONG A SHARP FLAT PLATE WITH A STRONG INDUCED PRESSURE FIELD

George R. Inger,†
*Aerospace Corporation, El Segundo, Calif.*

63-442

## Abstract

This paper presents a theoretical study of the effect of a strong self-induced pressure field on nonequilibrium hypersonic boundary layer flow along a sharp flat plate in a dissociating diatomic gas. An analytical solution describing the nearly frozen nonequilibrium flow near the leading edge is presented which explicitly shows the effects of the induced pressure field in the case of strong interaction, including the back effect of the growing dissociation level on the induced pressure field itself. Furthermore, an approximate solution is also obtained which applies throughout the nonequilibrium flow regime. Numerical examples for distributions of the maximum atom concentration, temperature, induced pressure, and heat transfer along the plate are given for various surface temperatures and representative hypersonic flight conditions. These results show, for example, that the induced pressure field can increase the degree of dissociation over a 10-ft run of plate by a factor of three to four or more at flight conditions of practical interest. Correspondingly, the induced pressures downstream of the leading edge are decreased below those computed for a frozen boundary layer, although this reduction is less than 20 per cent unless the wall temperature is very high. Examination of the results, however, indicates that the fully viscous flow region very near the leading edge acts to reduce the induced pressure field effects predicted by strong interaction theory and can play an important part in determining the nonequilibrium dissociation history along the plate.

## Introduction

Boundary-layer induced pressure fields have been heretofore neglected in analyses of nonequilibrium-dissociated and ionized boundary layer flows around slender aerodynamic bodies. Previous investigations concerning the interaction between an induced pressure field and high temperature real gas effects have been confined to the limiting cases of either chemically frozen or completely equilibrium dissociated gas flows.[1,2] However, strong self-induced pressures near the leading edge of such bodies do exist in just those low Reynolds number flight regimes which also favor a substantial departure from equilibrium within the boundary layer over an appreciable extent of the body. Therefore, since the early dissociation and ionization rates in such flows increase directly as the pressure, it is clear that a neglect of the induced pressure field could significantly underestimate the degree of dissociation and ionization in the flow field surrounding high altitude re-entry bodies.

To obtain some insight to this problem, this paper presents a theory of the nonequilibrium hypersonic boundary layer along a sharp flat plate in the presence of a strong induced pressure field for the case of a dissociating diatomic gas. The analysis employs the usual boundary layer equations in conjunction with a first order, strong interaction model of the induced pressure field based on hypersonic small disturbance theory. This appears to be a logical first step in appraising both the effect of induced pressure fields on the nonequilibrium boundary layer around slender aerodynamic bodies and the possible influence of the fully viscous flow region very near the leading edge on this nonequilibrium flow.

The simplifying assumptions and basic formulation of the problem are first given for the general case of a nonequilibrium-dissociating boundary layer flow of diatomic gas along a flat plate with a strong induced pressure field and with either a completely catalytic or perfectly noncatalytic surface. Then, based on the fact that atom recombination has a negligible effect on the nonequilibrium relaxation in the boundary layer except very near equilibrium,[3,4] an analytical solution is obtained which describes the nonsimilar chemical behavior in the nearly frozen region near the leading edge of the plate. By taking advantage of the exponential dependence of the dissociation rate on the temperature, a simple, closed form approximation to this first order solution is also derived. Furthermore, an approximate solution is given for arbitrary reaction rate (including recombination) throughout the nonequilibrium flow regime by performing a nonlinear, local extrapolation of the nearly frozen solution. Numerical examples of the theory for various surface temperatures and representative hypersonic flight conditions are then presented and discussed. Finally, the significance of the fully viscous region very near the plate leading edge will be examined in connection with these results.

## Formulation of the Problem

Consider laminar nonequilibrium boundary layer flow along a sharp flat plate immersed at zero angle of attack in a hypersonic stream of diatomic gas (Fig. 1). The plate has a uniform but arbitrary wall temperature and is either completely catalytic or perfectly noncatalytic with respect to atom recombination. The local inviscid flow in the thin layer between the shock envelope and the edge of the boundary layer is assumed to be one of small hypersonic disturbance ($u_e \simeq u_\infty$, $\sin^2\sigma << 1$) and to be chemically frozen. With respect to the flow in the boundary layer, one adopts as a matter of convenience the frequently-employed simplifying assumptions $Pr = Le = 1$, $\rho\mu = \text{constant} = \rho_e\mu_e = \rho_\infty\mu_\infty C_\infty(p_e/p_\infty)$, where $C_\infty$ is the Chapman-Rubesin constant, and $\tau_p = \text{constant}$. Moreover, following other investigators,[5,6,7] the pressure gradient term in the momentum equation is neglected and the velocity profile is taken to be independent of the solution to the energy and species conservation equations. This approximation, which can be justified theoretically when either the shock density ratio is very small[7,8] or the wall is highly cooled,[5,6] has but a minor effect on the nonequilibrium reaction effects of interest here.

INGER-2

† Member of the Technical Staff, Aerodynamics and Propulsion Research Laboratory.

Then, in terms of the well-known similarity coordinates

$$\left.\begin{aligned} \eta &= \frac{u_e}{\sqrt{2\xi}} \int_0^y \rho \, dy \\ \xi &= \rho_\infty \mu_\infty C_\infty u_\infty \int_0^x \left(\frac{p_e}{p_\infty}\right) dx \equiv \xi_o \int_0^x \frac{p_e}{p_\infty} \, dx \end{aligned}\right\} \quad (1)$$

the governing diffusion and energy equations for a nonequilibrium-dissociating boundary layer of diatomic gas can be written as

$$f \frac{\partial a}{\partial \eta} + \frac{\partial^2 a}{\partial \eta^2} - 2f' \xi \frac{\partial a}{\partial \xi} = -\Gamma(\xi) \cdot [D(a,T) - R(a,T)] \quad (2)$$

$$f \frac{\partial g}{\partial \eta} + \frac{\partial^2 g}{\partial \eta^2} - 2f' \xi \frac{\partial g}{\partial \xi} = 0 \quad (3)$$

where

$$\Gamma(\xi) = \underbrace{\frac{2k_r'(p_{at}/\Re_u)^2 (p_\infty/p_{at}) e^A}{T_{r,1}^2 u_\infty}}_{\Gamma_o} \cdot \frac{\xi(p_e/p_\infty)}{d\xi/dx} = \Gamma_o \frac{\xi}{\xi_o} \quad (4)$$

$$D(a,T) = \left(\frac{T}{T_{r,1}}\right)^{\omega-2} (1-a) \left(\frac{T}{T_{r,2}}\right)^S \exp\left(-\frac{T_d}{T}\right) \quad (5)$$

$$R(a,T) = \left(\frac{T}{T_{r,1}}\right)^{\omega-2} \left(\frac{4p_\infty/p_{at}}{e^A}\right) \cdot \frac{(p_e/p_\infty) a^2}{1+a} \quad (6)$$

$$g \equiv \frac{h_s}{h_{s,e}} = \frac{\bar{c}_p T + a h_d + (u_\infty^2/2)(f')^2}{\bar{c}_p T_e + a_\infty h_d + (u_\infty^2/2)} \quad (7)$$

Here, $f(\eta)$ is the Blasius function $[u/u_e \equiv f'(\eta)]$, $k_r'(T/T_{r,1})^\omega$ is the recombination rate constant, $T_{r,1}$ and $T_{r,2}$ are reference temperatures, S and A are constants, $p_{at}$ is atmospheric pressure, a is the atom mass fraction, $h_d$ is the dissociation energy per unit mass, and $T_d = h_d/\Re_m$ is a dissociation temperature of the molecules. The parameter $\Gamma(\xi)$ is a characteristic local (convection time/dissociation time) ratio for the boundary layer, while the functions $D(a,T)$ and $R(a,T)$ constitute the dissociation and recombination rate distributions, respectively, across the boundary layer. These functions have the important property that $D_{EQ} \equiv R_{EQ}$ in the limiting case of equilibrium flow. However, R is negligible in comparison to D throughout most of the nonequilibrium boundary layer flow regime along the plate except very close to equilibrium.[4]

The boundary conditions to be imposed on the solution to the foregoing equations are as follows. At the outer edge of the boundary layer (implicitly regarded here as distinct from the shock envelope), $a(\infty,\xi) = a_e = a_\infty$, $g(\infty,\xi) = 1$ and $f'(\infty) = 1$. At the body surface, $f(0) = f'(0) = 0$, either $T(0,\xi) = T_w =$ constant or $\dot{q}_w = 0$ (adiabatic wall), and either $a(0,\xi) = 0$ and $g(0,\xi) \equiv g_w = \bar{c}_p T_w/h_{s,e}$ for a completely catalytic surface* or $\partial a/\partial\eta(0,\xi) = 0$ {with $g(0,\xi) = g_w + [a(0,\xi)h_d]/h_{s,e}$ unknown} for the opposite extreme of a perfectly noncatalytic surface. In terms of the total enthalpy profile, the heat transfer rate $\dot{q}_w$ is given by the expression

$$\frac{\sqrt{2}\,(2\dot{q}_w/u_\infty^2)}{\sqrt{\xi_o}} \equiv Q_w = \frac{p_e/p_\infty}{\sqrt{\xi/\xi_o}} \frac{\partial g}{\partial \eta}(0,\xi) \cdot (1 + H_\infty) \quad (8)$$

where $H_\infty = 2a_\infty h_d/u_\infty^2$.

Formulation of the problem is completed by providing an equation for the displacement thickness distribution, $\delta^*(x)$, of the nonequilibrium boundary layer and by specifying an appropriate relationship between the induced pressure field and $d\delta^*/dx$. Consistent with the assumption of a small disturbance, hypersonic inviscid flow, the following expression for $d\delta^*/dx$ can be derived from the basic definition $\rho_e u_e \delta^* \equiv \int_0^\infty (\rho_e u_e - \rho u)dy$ upon neglecting the molecular weight variation in $\rho/\rho_e$ (which has a small effect in the present study) and using both the thermal equation of state and Eq. (7):

$$M_\infty \frac{d\delta^*}{dx} \equiv K^* = \left(\frac{\bar{\gamma}_\infty - 1}{2}\right) \bar{\chi}_\infty \sqrt{\frac{\phi(x)}{2(p_e/p_\infty)}} \cdot I(x)\left[1 + n(x) + \frac{x}{\phi}\frac{d\phi}{dx} + \frac{2x}{I}\frac{dI}{dx}\right] \quad (9)$$

where $\bar{\gamma}$ is the frozen specific heat ratio, $\bar{\chi}_\infty \equiv M_\infty^3 \sqrt{C_\infty/Re_{\infty,x}}$ is the usual viscous interaction parameter,

$$\phi(x) \equiv \frac{\int_0^x (p_e/p_\infty)dx}{(p_e/p_\infty)x} \quad (10)$$

*The heterogeneous dissociation rate on the surface is assumed negligible in comparison to the corresponding heterogeneous recombination rate.

$$n(x) \equiv -\frac{x}{p_e}\frac{dp_e}{dx} \tag{11}$$

and

$$I \equiv (1+H_\infty)\int_0^\infty [g-(f')^2]d\eta - H_\infty\int_0^\infty [1-(f')^2]d\eta - \frac{2h_d}{u_\infty^2}\int_0^\infty (a-a_\infty)d\eta \tag{12}$$

It is seen that the term I(x) contains the combined effects of viscous dissipation heating, inviscid flow dissociation, and nonequilibrium dissociation within the boundary layer on the local mass flow deficiency due to the boundary layer. The local pressure field will be related to $d\delta^*/dx$ by the tangent wedge approximation for the hypersonic small disturbance inviscid flow. In particular, for the case of strong interaction ($K^* \gg 1$) that is of prime interest here, this relation takes the form:[9]

$$\frac{p_e}{p_\infty} \simeq 1 + \frac{\bar{\gamma}_\infty(\bar{\gamma}_\infty+1)}{2}(K^*)^2 \tag{13}$$

Now, Eq. (13) underestimates the induced pressure in the region of moderate-to-weak interaction [$p_e/p_\infty - 1 \lesssim 0(1)$] downstream of the leading edge, since it neglects terms of order $K^*$ which eventually become important in this region. However, this is actually conservative for the present purpose of appraising the effect of the induced pressure field on the nonequilibrium relaxation in the boundary layer. Moreover, it will be seen that the significant effects of the induced pressure field on this relaxation occur almost entirely in the strong interaction region.

The general solution to Eqs. (2), (3), (7), (10) and (13) is a formidable mathematical task, involving a two point boundary value problem for two partial differential equations (one of which is highly nonlinear) that is coupled to a set of nonlinear ordinary differential equations. Even if one reduces Eqs. (2) and (3) to ordinary differential equations by assuming local similarity for the nonequilibrium boundary layer (i.e., neglecting the $\partial/\partial\xi$ terms a priori), a numerical solution on a digital computer is still required. However, a very useful insight to the main physical features of the problem can be obtained by first studying the case of nearly frozen nonequilibrium flow, where an analytical solution can be obtained in the presence of a strong induced pressure field. Moreover, this first order nonequilibrium boundary layer flow analysis also can be used in constructing an approximate, local nonequilibrium solution for arbitrary values of the reaction rate.

## Nearly Frozen Nonequilibrium Flow

Dissociation within the hypersonic boundary layer along the plate is instigated by the high temperatures resulting from viscous dissipation heating. At the leading edge where the boundary layer is chemically frozen, there exists an initial distribution of the dissociation rate per unit distance along the plate (with a pronounced maximum at the maximum frozen temperature) which initiates a dissociative relaxation toward equilibrium with increasing distance downstream of the leading edge. The recombination rate across the boundary layer in this highly nonequilibrium flow region is completely negligible by comparison unless $a_\infty$ is extremely close to unity.

### Series Method

Sufficiently near the leading edge, where the deviations from chemically frozen flow are small, the effect of chemical reaction on the boundary layer is related to the dissociation rate distribution based on frozen flow conditions and directly proportional to the local nonequilibrium flow parameter $\Gamma(\xi)$.[4] Therefore, one can assume solutions to Eqs. (2) and (3) of the form

$$a(\eta,\xi) = a_F(\eta) + \Gamma(\xi)\cdot a_I(\eta) \tag{14a}$$

$$g(\eta,\xi) = g_F(\eta) + \Gamma(\xi)\cdot g_I(\eta) \tag{14b}$$

$$T(\eta,\xi) = T_F(\eta) + \Gamma(\xi)\cdot T_I(\eta) \tag{14c}$$

where F is the frozen flow solution and I is the first order perturbations due to nonequilibrium reaction. By substituting Eqs. (14a, b, c) into Eqs. (2) and (3), equating to zero the net coefficient of each power of $\Gamma$, dropping second and higher order terms in $\Gamma$, and neglecting the effect of gas-phase recombination, one obtains the following two sets of relations governing the frozen flow and the first order reaction perturbations, respectively:

$$fa_F' + a_F'' = 0 \tag{15}$$

$$fg_F' + g_F'' = 0 \tag{16}$$

with

$$T_F = g_F T_e + \frac{h_d}{\bar{c}_p}(g_F a_\infty - a_F) + \frac{u_\infty^2}{2\bar{c}_p}[g-(f')^2] \tag{17}$$

and

$$f a_I' + a_I'' - 2f' a_I = -D_F(a_F, T_F) \tag{18}$$

$$f g_I' + g_I'' - 2f' g_I = 0 \tag{19}$$

with

$$T_I = \frac{h_{s,e} g_I - h_d a_I}{\bar{c}_p} \tag{20}$$

The corresponding boundary conditions become $a_F(\infty) = a_\infty$, $g_F(\infty) = 1$, $a_I(\infty) = g_I(\infty) = T_I(\infty) = 0$ with either $a_F(0) = a_I(0) = 0$ or $a_F'(0) = a_I'(0) = 0$. Also, for a fixed wall temperature, $T_w$, one has $T_F(0) = T_w$, $g_F(0) = g_w + [a_F(0)h_d]/h_{s,e}$, $T_I(0) = 0$ and $g_I(0) = [a_I(0)h_d]/h_{s,e}$; however, in the special case of an adiabatic wall, one has instead simply the two conditions $g_F'(0) = g_I'(0) = 0$. It should be noted that the equations governing the first order nonequilibrium effects do not involve the local pressure and can therefore be solved independently of the particular relationship, such as (13), assumed in calculating $p_e/p_\infty$. This fortunate situation arises from the fact that the entire effect of the pressure field on the boundary layer reaction rate for nearly frozen flow is implicit in the coordinate $\xi$ when gas-phase recombination is neglected. Therefore, since $\Gamma \sim \xi$ and $\xi(\partial/\partial\xi) \sim \Gamma$, the pressure simply cancels out (residing solely in $\Gamma$) in obtaining Eqs. (18) and (19).

Relations governing the induced pressure field for strong interaction, including the first order back effect of nonequilibrium dissociation within the boundary layer, can now be derived. First, by substituting expansions (14a) and (14b) into Eq. (12), the displacement thickness integral I can be written as

$$I = I_F + \Gamma I_I \tag{21}$$

where

$$I_F = (1 + H_\infty)\int_0^\infty [g_F - (f')^2]d\eta - H_\infty \int_0^\infty [1 - (f')^2]d\eta - \frac{2h_d}{u_\infty^2}\int_0^\infty (a_F - a_\infty)d\eta \tag{22a}$$

$$I_I = (1 + H_\infty)\int_0^\infty g_I\, d\eta - \frac{2h_d}{u_\infty^2}\int_0^\infty a_I\, d\eta \tag{22b}$$

are constants which can be evaluated once Eqs. (15)-(19) are solved. Then, by analogy with Eqs. (14) and (21), one assumes solutions for $K^*$ and $p_e/p_\infty$ of the form

$$K^* = K_F^*\left(1 + K_I^* \frac{I_I}{I_F}\Gamma\right) \tag{23}$$

$$\frac{p_e}{p_\infty} = \left(\frac{p_e}{p_\infty}\right)_F \left(1 + P_I \frac{I_I}{I_F}\Gamma\right) \tag{24}$$

where $K_I^*$ and $P_I$ depend on the frozen flow solution. Substituting Eqs. (23) and (24) into (9) and (13) and dropping second and higher terms in $\Gamma$, the following two sets of relations governing the frozen boundary layer induced pressure field and the nonequilibrium perturbation thereof, respectively, are obtained:

$$K_F^* = \left(\frac{\bar{\gamma}_\infty - 1}{2}\right)\bar{x}_\infty \sqrt{\frac{\phi_F}{2(p_e/p_\infty)_F}}\,(1 + n_F) I_F \tag{25a}$$

$$\left(\frac{p_e}{p_\infty}\right)_F = 1 + \frac{\bar{\gamma}_\infty(\bar{\gamma}_\infty + 1)}{2}\left(K_F^*\right)^2 \tag{25b}$$

and

$$K_I^* = \frac{(p_e/p_\infty)_F}{\bar{\gamma}_\infty(\bar{\gamma}_\infty + 1)\left(K_F^*\right)^2} P_I \tag{26a}$$

$$P_I = \left[\left(\frac{1 + n_F}{3 - n_F}\right)\frac{(p_e/p_\infty)_F}{\bar{\gamma}_\infty(\bar{\gamma}_\infty + 1)\left(K_F^*\right)^2} + 1 - \frac{z_F}{2}\right]^{-1} \tag{26b}$$

where

$$z_F \equiv \frac{\int_0^x (p_e/p_\infty)^2 x\, dx}{(p_e/p_\infty)x\int_0^x (p_e/p_\infty)dx} \tag{27}$$

Corresponding to the pressure field (24), it is also found that

$$\phi = \phi_F\left[1 + P_I(1 - z_F)\frac{I_I}{I_F}\Gamma\right] \tag{28}$$

and

$$\left.\begin{aligned} \Gamma &= \Gamma_F \Big/ \left(1 - \Gamma_F z_F P_I \frac{I_I}{I_F}\right) \\ \Gamma_F &\equiv \Gamma_o \phi_F (p_e/p_\infty)_F^{\,x} \end{aligned}\right\} \qquad (29)$$

which prove useful later. Note that in deriving Eqs. (26), (28), and (29), the parameters $\phi_F$, $n_F$ and $z_F$ were each taken to be constant. This is indeed exact in the limit of strong interaction ($\bar{\chi}_\infty >> 1$) and also remains a good approximation even for arbitrary values of $\bar{\chi}_\infty$ since these parameters are usually rather slowly varying functions of $X$ in the general case.[10]

Finally, the heat transfer to the plate can be written to the first order in $\Gamma$ upon substitution of Eqs. (14b), (24), and (28) into (8) as follows:

$$Q_w = (1 + H_\infty)\sqrt{\frac{(p_e/p_\infty)_F}{\phi_F x}} \left\{ g_F'(0) + \Gamma\left[ g_I'(0) + \left(\frac{2 - z_F}{2}\right) P_I g_F'(0) \frac{I_I}{I_F} \right] \right\} \qquad (30)$$

The two terms inside the square bracket multiplying $\Gamma$ represent the first order effect of nonequilibrium reaction on the enthalpy profile and the influence of the corresponding back effect of this reaction on the induced pressure field, respectively.

Frozen Flow Solution

Solutions to Eqs. (15) and (16) for the stipulated boundary conditions are easily obtained by direct integration. Noting that $ff'' + f''' = 0$, the atom concentration distribution is found to be

$$\left.\begin{aligned} \alpha_F(\eta) &= \alpha_\infty f'(\eta) \quad , \quad \text{catalytic wall} \\ &= \alpha_\infty \quad , \quad \text{noncatalytic wall} \end{aligned}\right\} \qquad (31)$$

Correspondingly, the frozen flow total enthalpy profile is as follows:

$$\left.\begin{aligned} g_F(\eta) &= g_w + (1 - g_w) f' + \frac{h_d}{h_{s,e}} (1 - f') \alpha_F(0) \\ g_F'(0) &= \left[ 1 - g_w - \frac{h_d \alpha_F(0)}{h_{s,e}} \right] f''(0) \end{aligned}\right\} \qquad (32)$$

Then, for a fixed wall temperature, Eq. (17) yields

$$T_F(\eta) = T_w + (T_e - T_w) f' + \frac{u_\infty^2}{2\bar{c}_p} f'(1 - f') \qquad (33)$$

regardless of the surface catalycity.* However, in the special case of an adiabatic wall, the temperature profile depends on the surface catalycity when $\alpha_\infty > 0$:

$$\left.\begin{aligned} T_F(\eta) &= T_e + \frac{u_\infty^2}{2\bar{c}_p} (1 - f')(1 + f') \\ &\quad + \frac{h_d}{\bar{c}_p} (1 - f')[\alpha_\infty - \alpha_F(0)] \\ T_F'(0) &= - \frac{h_d}{\bar{c}_p} f''(0)[\alpha_\infty - \alpha_F(0)] \end{aligned}\right\} \qquad (34)$$

Equations (34) show that in the presence of a dissociated inviscid flow the frozen temperature gradient in the gas at an adiabatic wall does not vanish unless the surface is perfectly noncatalytic.

Typical distributions of the frozen boundary layer temperature and the corresponding dissociation rate function $D_F(\alpha_F, T_F)$ are presented in Fig. 2. It is seen from these curves that the dissociation rate is mainly concentrated in a rather narrow band centered on the position $\eta = \eta^*$ of the maximum in the frozen temperature profile. The value of $\eta^*$ is determined from the following relation obtained by setting $T_F'(\eta^*) = 0$ in Eq. (33):

$$f'(\eta^*) = \frac{1}{2} + \frac{\bar{c}_p (T_e - T_w)}{u_\infty^2} \quad , \quad f'(\eta^*) < 1 \qquad (35)$$

Turning to the calculation of the self-induced pressure field acting on the frozen boundary layer, one first evaluates the displacement thickness integral $I_F$ from solutions (31) and (32) with the following result:[7]

$$I_F = \int_0^\infty f'(1 - f')d\eta + \frac{2\bar{c}_p T_w}{u_\infty^2} \int_0^\infty (1 - f')d\eta \simeq 0.470 + 1.22 \left( \frac{2\bar{c}_p T_w}{u_\infty^2} \right) \qquad (36)$$

*Here, to be consistent with the hypersonic small disturbance approximations and chemically frozen flow conditions employed, one must take $T_e = T_\infty$.

To the present order of approximation, this relation gives no effect of surface catalycity on the induced pressure field, regardless of the inviscid flow dissociation level. Now, the algebraic Eqs. (25) can be solved for $p_e/p_\infty$ with the following result in the strong interaction case:

$$\left(\frac{p_e}{p_\infty}\right)_F \simeq 1 + \frac{3}{8}(\bar{\gamma}_\infty - 1)\sqrt{2\bar{\gamma}_\infty(\bar{\gamma}_\infty + 1)}I_F\bar{\chi}_\infty$$

$$\equiv 1 + p_{o,F}\bar{\chi}_\infty \qquad (37)$$

Based on Eq. (37), the parameters $\phi_F$, $n_F$ and $z_F$ defined above take the approximate values

$$\phi_F \simeq \frac{2p_{o,F}\bar{\chi}_\infty + 1}{p_{o,F}\bar{\chi}_\infty + 1} \left\{ \begin{array}{l} = 2 \text{ for } \bar{\chi}_\infty \gg 1 \\ = 1 \text{ for } \bar{\chi}_\infty \to 0 \end{array} \right\} \qquad (38)$$

$$n_F \simeq \frac{1}{2}\left(\frac{p_{o,F}\bar{\chi}_\infty}{1 + p_{o,F}\bar{\chi}_\infty}\right) \left\{ \begin{array}{l} = 1/2 \text{ for } \bar{\chi}_\infty \gg 1 \\ = 0 \quad \text{for } \bar{\chi}_\infty \to 0 \end{array} \right\} (39)$$

$$z_F \simeq \frac{1}{2} \qquad (40)$$

Correspondingly, the parameter $P_I$ defined by Eq. (26b) can be expressed in the more explicit form

$$P_I \simeq \frac{20}{21}\left(\frac{p_{o,F}^2\bar{\chi}_\infty^2}{p_{o,F}^2\bar{\chi}_\infty^2 + 4/21}\right) \left\{ \begin{array}{l} = 20/21 \text{ for } \bar{\chi}_\infty \gg 1 \\ = 0 \text{ for } \bar{\chi}_\infty \to 0 \end{array} \right\} (41)$$

It appears from inspection of these approximate relations and their limiting values (which are exact) that $\phi_F$, $n_F$, $P_I$ and (especially) $z_F$ are slowly varying parameters along the plate. In fact, $\phi_F$, $n_F$ and $P_I$ vary more gradually with $x$ than is indicated by Eqs. (38) - (41), since these equations neglect terms of order $K^*$ compared to $(K^*)^2$ and therefore reflect too rapid a presure decay downstream of the strong interaction region.

The frozen boundary layer heat transfer including the effect of the induced pressure field becomes

$$Q_{w,F} \simeq \frac{1 + p_{o,F}\bar{\chi}_\infty}{\sqrt{(2p_{o,F}\bar{\chi}_\infty + 1)x}} \left\{ 1 + \frac{2h_d}{u_\infty^2}[\alpha_\infty - \alpha_F(0)] - \frac{2\bar{c}_p T_w}{u_\infty^2} \right\} f''(0) \qquad (42)$$

When $\bar{\chi}_\infty \gg 1$, Eq. (42) yields the well-known strong-interaction result[11] $Q_{w,F} \sim \sqrt{\bar{\chi}_\infty/x} \sim x^{-3/4}$; whereas, in the absence of an induced pressure field, the classical result $Q_{w,F} \sim x^{-1/2}$ is obtained.

First Order Solution

Equation (18), which governs the first order nonequilibrium atom concentration within the boundary layer, has been previously treated by Rae[4] in his analysis of the nonequilibrium problem for the flat plate without an induced pressure field. The solutions are readily obtained by standard methods in terms of the known solution $s(\eta)$ to the associated homogeneous equation

$$fs' + s'' - 2f's = 0 \; ; \quad s(0) = 1 \; ; \quad s'(0) = 0 \qquad (43)$$

These solutions are

$$\left. \begin{array}{l} \alpha_I(\eta) = \mathcal{I}(\infty)s(\eta)[V_s(\eta) - i(\eta)] \\ \alpha_I'(0) = \mathcal{I}(\infty)f''(0)/v_s(\infty) \end{array} \right\} \text{ catalytic wall} \qquad (44)$$

$$\left. \begin{array}{l} \alpha_I(\eta) = \mathcal{I}(\infty)s(\eta)[1 - i(\eta)] \\ \alpha_I(0) = \mathcal{I}(\infty) \end{array} \right\} \text{ noncatalytic wall} \qquad (45)$$

where

$$v_s(\eta) \equiv \int_0^\eta \frac{f''(\eta)}{s^2(\eta)}\, d\eta \qquad (46a)$$

$$V_s(\eta) \equiv \frac{v_s(\eta)}{v_s(\infty)} \qquad (46b)$$

$$\mathcal{I}(\eta) \equiv \int_0^\eta \frac{f''(\eta)}{s^2(\eta)}\left[\int_0^\eta \frac{s(\eta)D_F(\eta)d\eta}{f''(\eta)}\right] d\eta \qquad (47a)$$

$$i(\eta) \equiv \frac{\mathcal{I}(\eta)}{\mathcal{I}(\infty)} \qquad (47b)$$

Plots of $s(\eta)$ and $v_s(\eta)$, taken from Ref. 4, are given in Fig. 3. Some typical distributions of the normalized reaction rate integral, $i(\eta)$, corresponding to the dissociation rate profiles shown in Fig. 2 are presented in Fig. 4. It is seen that the ratio $i(\eta)$ is relatively unaffected by the reaction rate distribution. Moreover, it was found that unless the free stream is very highly dissociated or $T_w/T_o > 0.25$ with $\alpha_\infty > 0$, $i(\eta)$ may be taken as independent of the surface catalycity. INGER-6

As pointed out in Ref. 4, a very useful closed form approximation to the overall reaction rate integral $\mathcal{I}(\infty)$ can be obtained by the method of steepest descent[12] for highly dissipative boundary layer flows with a pronounced temperature maximum in the boundary layer. Expanding Eq. (47a) into two single integrals with an integration by parts, and then using this method in evaluating the integrals (see Refs. 4 and 12 for details), one can obtain the following analytical expression for $\mathcal{I}(\infty)$:

$$\left.\begin{aligned}\mathcal{I}(\infty) &\simeq \frac{s(\eta^*)}{f''(\eta^*)}\sqrt{\pi}\,\beta^*[v_s(\infty) - v_s(\eta^*)] \\ &\cdot \left[\frac{1 + \operatorname{erf}(\eta^*/\beta^*)}{2}\right] \cdot D_F(\eta^*) \\ &\equiv F^* \cdot D_F(\eta^*)\end{aligned}\right\} \quad (48)$$

where

$$(\beta^*)^2 \equiv \frac{2\bar{c}_p T_F^2(\eta^*)}{u_\infty^2 T_D [f''(\eta^*)]^2} \quad (49)$$

Equation (48) can be thought of as representing the overall reaction rate integral by the product of the dissociation rate at the maximum frozen temperature and a form factor accounting for the integrated effect of reaction across the boundary layer as modified by convection and diffusion. Comparison with exact numerical values shows that this approximation represents the functional dependence of $\mathcal{I}(\infty)$ on the various physical parameters reasonably well but underestimates the magnitude by approximately a factor of two for highly cooled flows.[13] Corresponding to Eq. (48), the steepest descent method also gives

$$\mathcal{I}(\eta^*) \simeq 0 \quad (50)$$

which in turn yields the following solutions for the maximum atom concentration perturbations:

$$\left.\begin{aligned}\alpha_{I,\text{non-cat}}(\eta^*) &\simeq s(\eta^*)\mathcal{I}_{\text{non-cat}}(\infty) \simeq s(\eta^*)\alpha_I(0) \\ \alpha_{I,\text{cat}}(\eta^*) &\simeq s(\eta^*)V_s(\eta^*)\mathcal{I}_{\text{cat}}(\infty) \\ &\simeq \left[\frac{1 - \alpha_\infty f'(\eta^*)}{1 - \alpha_\infty}\right] V_s(\eta^*)\alpha_{I,\text{non-cat}}(\eta^*)\end{aligned}\right\} \quad (51)$$

Now, as indicated in Fig. 4, the exact values of $\mathcal{I}(\eta^*)$ for highly cooled flows are more nearly equal to $1/2\ \mathcal{I}(\infty)$, so that Eq. (50) is clearly a rather poor approximation in itself for such flows. However, since the corresponding approximation (48) also underestimates $\mathcal{I}(\infty)$ by roughly a factor of two, Eqs. (44) and (45) show that the two errors tend to cancel each other in determining $\alpha_I(\eta)$. The resulting approximate solutions (51) appear to be satisfactory for engineering purposes.[4,13]

Turning to the total enthalpy perturbation in Eq. (20), the solution is readily found by using (43) to be

$$\left.\begin{aligned}g_I(\eta) &= \frac{h_d}{h_{s,e}}\alpha_I(0)s(\eta)[1 - V_s(\eta)] \\ g_I'(0) &= -\frac{h_d}{h_{s,e}}\alpha_I(0)\frac{f''(0)}{v_s(\infty)}\end{aligned}\right\} \quad (52)$$

for a fixed wall temperature, and $g_I(\eta) = 0$ for an adiabatic wall. As expected, (52) shows that there is no effect of chemical reaction on the total enthalpy profile for a completely catalytic wall when $Le = 1$.[6] From Eq. (20), the corresponding temperature distribution perturbations for fixed wall temperature are

$$\left.\begin{aligned}T_{I,\text{cat}}(\eta) &= -\frac{h_d}{\bar{c}_p}\alpha_{I,\text{cat}}(\eta) \\ &= -\frac{h_d}{\bar{c}_p}\mathcal{I}_{\text{cat}}(\infty)s(\eta)[V_s(\eta) - i(\eta)]\end{aligned}\right\} \quad (53a)$$

$$\left.\begin{aligned}T_{I,\text{non-cat}}(\eta) &= \frac{\mathcal{I}_{\text{non-cat}}(\infty)}{\mathcal{I}_{\text{cat}}(\infty)} \cdot T_{I,\text{cat}}(\eta) \\ &\simeq \left[\frac{1 - \alpha_\infty}{1 - \alpha_\infty f'(\eta^*)}\right] T_{I,\text{cat}}(\eta)\end{aligned}\right\} \quad (53b)$$

these two solutions being identical in the case of an undissociated free stream. On the other hand, for an adiabatic wall, one finds a more significant effect of surface catalycity on the nonequilibrium temperature field:

$$\left.\begin{aligned}T_{I,\text{cat}}(\eta) &= -\frac{h_d}{\bar{c}_p}\alpha_{I,\text{cat}}(\eta) \\ \text{with} \\ T_I'(0) &= -\frac{h_d}{\bar{c}_p}\alpha_{I,\text{cat}}'(0)\end{aligned}\right\} \quad (54a)$$

$$\left.\begin{aligned}T_{I,\text{non-cat}}(\eta) &= -\frac{h_d}{\bar{c}_p}\alpha_{I,\text{non-cat}}(\eta) \\ &= -\frac{h_d}{\bar{c}_p}\mathcal{I}_{\text{non-cat}}(\infty)s(\eta)[1 - i(\eta)] \\ \text{with} \\ T_I'(0) &= 0\end{aligned}\right\} \quad (54b)$$

It is seen that the temperature gradient at an adiabatic, completely catalytic wall is not zero in the presence of nonequilibrium dissociation, since there must be a conduction of heat in the gas away from the wall which just balances the diffusion of heat from the gas to the wall.

The first order nonequilibrium solution is completed by evaluating the displacement thickness perturbation $I_I$. Substituting the foregoing solutions for $a_I(\eta)$ and $g_I(\eta)$ into Eq. (22b), one finds

$$I_{I,\,cat} = -\frac{2h_d}{u_\infty^2}\,\mathcal{J}_{cat}(\infty)\int_0^\infty s(\eta)[V_s(\eta) - i(\eta)]d\eta$$

$$\equiv -\frac{2h_d}{u_\infty^2}\,\mathcal{J}_{cat}(\infty)\cdot I_{c,1} \qquad (55a)$$

$$I_{I,\,non\text{-}cat} = -\frac{2h_d}{u_\infty^2}\,\mathcal{J}_{non\text{-}cat}(\infty)\,I_{c,1}$$

$$\simeq\left[\frac{1 - a_\infty}{1 - a_\infty f'(\eta^*)}\right] I_{I,\,cat} \qquad (55b)$$

for fixed wall temperature, and

$$I_{I,\,cat} = -\frac{2h_d}{u_\infty^2}\,\mathcal{J}_{cat}(\infty) I_{c,1} \qquad (56a)$$

$$I_{I,non\text{-}cat} = -\frac{2h_d}{u_\infty^2}\,\mathcal{J}_{non\text{-}cat}(\infty)\int_0^\infty s(\eta)\cdot$$

$$\cdot[1 - i(\eta)]d\eta \equiv -\frac{2h_d}{u_\infty^2}\,\mathcal{J}_{non\text{-}cat}(\infty)\cdot I_{c,2} \qquad (56b)$$

for an adiabatic wall. The integrals $I_{c,1}$ and $I_{c,2} > I_{c,1}$ can be regarded as independent of the surface catalycity unless $a_\infty \to 1$ or $T_w/T_o > 0.25$ with $a_\infty > 0$. Consequently, the back effect of the nonequilibrium dissociation within the boundary layer on the self-induced pressure field is not significantly affected by the surface catalycity unless either the free stream is highly dissociated or the wall temperature is extremely large. Typical values of $I_{c,1}$ and $I_{c,2}$ are presented in Table 1.

## Summary of the Complete Solution

Let us now summarize the complete first order solutions obtained for the maximum atom concentration and corresponding temperature, the induced pressure field, and the heat transfer. For this purpose, the closed-form approximations for $a_I(\eta^*)$ and $\mathcal{J}(\infty)$ defined above will be employed (although this is of course not necessary). Thus, by substituting the foregoing perturbation solutions into the general expansions (14), (24), and (30), one obtains $T(\eta^*)$, $p_e/p_\infty$ and $Q_w$ in terms of the frozen flow solution and the nonequilibrium atom concentration for a fixed wall temperature as follows:

$$T(\eta^*) = T_F(\eta^*) - \frac{h_d}{\bar{c}_p}\left[j + (1 - j)V_s(\eta^*)\right]\cdot$$

$$\cdot\left[a(\eta^*) - a_F(\eta^*)\right] \qquad (57)$$

$$\frac{p_e}{p_\infty} = \left(\frac{p_e}{p_\infty}\right)_F\left\{1 - \left(\frac{2h_d}{u_\infty^2}\,P_I\,\frac{I_{c,1}}{I_F}\right)\cdot\right.$$

$$\left.\cdot\left[\frac{a(\eta^*) - a_F(\eta^*)}{\bar{s}^*}\right]\right\} \qquad (58)$$

$$Q_w = \sqrt{\frac{(p_e/p_\infty)_F}{\phi_F x}}\cdot$$

$$\cdot\left\{g'_F(0) - \frac{2h_d}{\bar{c}_p}\left[\frac{1 - j}{V_s(\infty)} + P\,\frac{I_{c,1}}{I_F}\,g'_F(0)\right]\cdot\right.$$

$$\left.\cdot\left[\frac{a(\eta^*) - a_F(\eta^*)}{\bar{s}^*}\right]\right\} \qquad (59)$$

where

$$\bar{s}^* \equiv s(\eta^*)\left\{1 + j[V_s(\eta^*) - 1]\right\} \qquad (60)$$

with $j = 0$ for a noncatalytic wall and $j = 1$ for a completely catalytic wall.* The corresponding solution for the atom concentration is given by

$$a(\eta^*) - a_F(\eta^*) = \Gamma\,\mathcal{J}(\infty)\bar{s}^* \qquad (61)$$

with

$$\Gamma = \Gamma_o\phi_F\left(\frac{p_e}{p_\infty}\right)_F x\cdot$$

$$\cdot\left\{1 - \left(\frac{2h_d}{u_\infty^2}\,z_F P_I\,\frac{I_{c,1}}{I_F}\right)\left[\frac{a(\eta^*) - a_F(\eta^*)}{\bar{s}^*}\right]\right\} \qquad (62)$$

*These solutions also apply to an adiabatic wall when the surface is completely catalytic and can be adapted to the noncatalytic case by simply replacing $I_{c,1}$ by $I_{c,2}$ and using $j = 1$ instead of $j = 0$ in Eq. (57).

and where $\mathfrak{f}(\infty)$ is given (approximately) by Eq. (48). These closed form solutions, which are correct to first order in $a(\eta^*) - a_F(\eta^*)$,* provide useful insight as to the behavior of a nonequilibrium-dissociating boundary layer with a self-induced pressure field. Near the leading edge of the plate, for example, Eqs. (61) and (62) show that the strong induced pressure field of the frozen boundary layer ($\bar{\chi}_\infty >> 1$, $\phi_F = 2$, $\Gamma \sim 2p_{o,F}\bar{\chi}_\infty x$) increases the atom concentration relative to the concentration predicted, neglecting the induced pressure field ($\bar{\chi}_\infty = 0$, $\phi_F = 1$, $\Gamma \sim x$) by a factor $2p_{o,F}\bar{\chi}_\infty x$. Correspondingly, Eq. (58) shows explicitly how the resulting back effect of the nonequilibrium dissociation on the boundary layer displacement thickness decreases the induced pressure below the local frozen flow value as the dissociation level grows with increasing distance from the leading edge. It is seen that this back effect grows as $\sqrt{x}$ near the leading edge for strong interaction. Similarly, Eq. (59) shows that the back effect on pressure also reduces the local heat transfer, in addition to the reduction caused by the enhanced wall enthalpy for the noncatalytic wall case. Further details of the first order solution will be discussed below in connection with some specific numerical examples.

## Extension to Arbitrary Reaction Rate

The foregoing analytical solution for $\Gamma(\xi) << 1$ is very helpful in understanding the effects of the induced pressure field and in analyzing the initial nonequilibrium flow near the leading edge. Nevertheless, this solution will clearly break down in the nonlinear relaxation region further downstream of the leading edge. Moreover, it does not prove fruitful to extend the first order analysis by carrying the series developments (14) to second order terms in $\Gamma$, since the resulting solutions are very complicated and have an extremely small radius of convergence. Consequently, an approximate, nonlinear method of carrying the nearly frozen solution forward throughout the entire nonequilibrium flow field, while avoiding exact numerical solutions of the basic, nonlinear differential equations, would be of interest.

Such a method was originally devised by Rae in Ref. 4 and subsequently adapted with success by the present author to several other problems involving nonequilibrium-dissociated viscous flows with both gas-phase and/or catalytic surface reactions.[14,15] The basic idea behind the method lies in the intuitive notion that the nearly frozen first order solution would still yield an essentially correct description of the nonequilibrium behavior in the nonlinear relaxation region downstream of the leading edge if the reaction rate were based on the local nonequilibrium state instead of being evaluated from the frozen flow solution. Therefore, one can seek an approximate solution throughout the relaxation region by performing an appropriate local extrapolation of the nearly frozen theory for small $\Gamma$ [$(a - a_F) \to 0$] whereby the <u>form</u> of this theory is carried forward to arbitrary $\Gamma$. Applying this idea to the present problem, then, one assumes that Eqs. (57)-(61), which are rigorously correct only for sufficiently small values of x, are in fact essentially the correct solution everywhere <u>provided</u> that the value of $\Gamma$ from Eq. (62) and the function $\mathfrak{f}(\infty)$ defined by Eq. (48) are both evaluated at the <u>local</u>, unknown values of $a(\eta^*)$, $T(\eta^*)$ and $p_e/p_\infty$. Thus, one adopts the following as an approximate solution for the nonequilibrium atom concentration (including an induced pressure field):

$$a(\eta^*) - a_F(\eta^*) \simeq \Gamma \bar{s}^* F^*[a(\eta^*), T(\eta^*)] \cdot \left\{ D[a(\eta^*), T(\eta^*)] - R\left[a(\eta^*), T(\eta^*), \frac{p_e}{p_\infty}\right]\right\} \tag{63}$$

with

$$F^*[a(\eta^*), T(\eta^*)] = \frac{s(\eta^*)[v_s(\infty) - v_s(\eta^*)]}{[f''(\eta^*)]^2} \cdot \sqrt{\frac{2\pi\bar{c}_p}{U_\infty^2 T_d}}\, T(\eta^*) \cdot \left\{1 + \operatorname{erf}\left[\frac{\eta^* f''(\eta^*)}{T(\eta^*)}\sqrt{\frac{u_\infty^2 T_d}{2\bar{c}_p}}\right]\right\} \tag{64}$$

$$D[a(\eta^*), T(\eta^*)] = \left[\frac{T(\eta^*)}{T_{r,1}}\right]^{\omega-2}[1 - a(\eta^*)] \cdot \left[\frac{T(\eta^*)}{T_{r,2}}\right]^s \exp\left[-\frac{T_d}{T(\eta^*)}\right] \tag{65}$$

$$R\left[a(\eta^*), T(\eta^*), \frac{p_e}{p_\infty}\right] = \left[\frac{T(\eta^*)}{T_{r,1}}\right]^{\omega-2}\left(\frac{4p_\infty/p_{at}}{e^A}\right) \cdot \left[\frac{(p_e/p_\infty)a(\eta^*)^2}{1 + a(\eta^*)}\right] \tag{66}$$

where $T(\eta^*)$ and $p_e/p_\infty$ are still given by Eqs. (57) and (58), respectively. Note that in writing Eq. (63), the complete net reaction rate function, including recombination, has been used. This is valid only when the local recombination rate is small compared to the dissociation rate, which indeed is found to be the case until nearly complete equilibration of the dissociation reaction is reached. Moreover, retention of the recombination term ensures that $a(\eta^*)$ will approach the proper functional dependence on $T(\eta^*)$ and $p_e/p_\infty$ as the solution tends toward equilibrium at sufficiently large values of x; since, as $x \to \infty$, the net reaction rate D - R in Eq. (63) correctly approaches zero.



*Strictly speaking, the second term in Eq. (62) should be dropped as second order in $a(\eta^*) - a_F(\eta^*)$ when used in Eq. (61). However, this relation for $\Gamma$ is by itself correct to first order in $a(\eta^*) - a_F(\eta^*)$ and will be used later in extending our solution to arbitrary degrees of dissociation.

The foregoing approximate solution involves a set of four simultaneous, nonlinear algebraic equations which are easily solved on a computer, using the first order nearly frozen flow analysis as a starting solution at small x. The corresponding local nonequilibrium heat transfer distribution can then be determined (approximately) by direct substitution into Eq. (59). Since this nonlinear solution gives the right initial behavior near the leading edge and also incorporates the correct qualitative behavior at large x, it should provide a fairly accurate description of the smooth, monotonic distributions of the unknowns along the plate expected in the present problem. Moreover, the proven usefulness of the extrapolation method in other problems, particularly in the plate problem treated in Ref. 4, suggests that it should provide reasonable solutions in the presence of an induced pressure field as well. To be sure, as Rae has pointed out, the method does not satisfactorily describe the boundary layer all the way to equilibrium in the case of a cold wall, and further comparisons with exact solutions are certainly needed to more fully define its accuracy and limitations. Nevertheless, it appears to be quite accurate over the very-highly nonequilibrium boundary layer flow region in the vicinity of the leading edge where the most significant induced pressures are expected to occur.

## Numerical Examples

### Discussion of Results

The main features of the present theory for a typical case are illustrated in Fig. 5, where distributions of $\alpha(\eta^*)$, $T(\eta^*)$, $p_e/p_\infty$ and $Q_w$, respectively, for the flow of oxygen over a cold, noncatalytic plate are shown with the induced pressure field both taken into account and neglected. Values of the parameters used in the present numerical examples are given in Table 2. To indicate the various operating effects, both the first order solution and the various contributions comprising the local nonlinear solution for each variable have been shown. It is seen that the first order solutions both with and without the induced pressure field describe only a rather small portion of the entire nonequilibrium flow region, significantly overestimating the (nonlinear) relaxation effects beyond a local dissociation level of roughly 10 per cent. With respect to the nonlinear solution for $\alpha(\eta^*)$, it is seen that the induced pressure field here increases the local maximum degree of dissociation in the boundary layer (relative to that predicted neglecting this field) by a factor ranging from two to three or more over the first 10 ft run of plate. This increase in $\alpha(\eta^*)$ also causes a pronounced reduction of the local maximum temperature (e.g., by 1300°K at $x = 10$ ft ) because of the large dissociation energy involved. The corresponding back effect of the nonequilibrium dissociation on the displacement thickness reduces the local induced pressure field about 20 per cent below that computed for a frozen boundary layer flow, resulting in a slightly more rapid pressure decay downstream of the leading edge. Also, Fig. 5(d) shows that the reduction in heat transfer caused by nonequilibrium dissociation grows more rapidly downstream of the leading edge when the induced pressure field is taken into account, with about half of this enhanced reduction resulting from the back effect on the pressure field itself. However, it is seen that this back effect has a negligible effect on both $\alpha(\eta^*)$ and $T(\eta^*)$ throughout the relaxation region, which was generally found to be the case in all the numerical examples presented here.

The effects of wall temperature and surface catalycity on the maximum atom concentration and induced pressure field solutions of Fig. 5 are shown in Fig. 6. Increasing wall temperature accelerates the relaxation toward equilibrium along the plate, since the corresponding increase in boundary layer temperature increases the local dissociation rate significantly through the exponential dependence of this rate on temperature. At the same time, the effect of the induced pressure field on the nonequilibrium boundary layer state is also increased because of the increase in displacement thickness with wall temperature. When $T_w/T_o \gtrsim 0.25$ at this flight condition, for example, strong interaction has a very large effect, increasing $\alpha(\eta^*)$ by an order of magnitude over the first foot of the plate while causing a decrease in the local pressure field itself through the back effect of this dissociation by nearly a factor of two. The surface catalycity does not have a large percentage effect on the local maximum atom concentration for a highly cooled wall; the value of $\alpha(\eta^*)$ for a completely catalytic surface is approximately 75 per cent of the value for a perfectly noncatalytic surface because of the loss of atoms by diffusion to (and recombination on) the wall that occurs in the former case. Nevertheless, this 25 per cent difference does become significant as the dissociation level grows along the plate, particularly with increased wall temperature. However, at least for values of $T_w/T_o \lesssim 0.25$, it is seen that the relative effect of the induced pressure field on the nonequilibrium behavior is relatively insensitive to the surface catalycity.

The effect of flight Mach number and altitude on the distributions of atom concentration and pressure along the plate are presented in Figs. 7 and 8, respectively, for a highly cooled noncatalytic wall. The influence of the induced pressure field is found to subside with decreasing Mach number at a given altitude because of the lower values of $\bar{\chi}_\infty$. Correspondingly, the boundary layer remains frozen over a greater extent of the plate due to the decrease in dissociation rate caused by reduced viscous dissipation heating within the boundary layer. At $M_\infty = 15$ and 200,000 ft altitude, for example, it is seen that the induced pressure field has a negligible effect on the dissociation chemistry of the boundary layer, the flow along the plate being essentially frozen to well over 100 ft downstream of the leading edge. On the other hand, an increase in altitude at fixed Mach number enhances the relative effect of the induced pressure field on the nonequilibrium dissociation within the boundary layer because of a lower Reynolds number, although the dissociation level itself is decreasing since the reduced ambient density decreases the dissociation rate ($\Gamma$). From the results presented in Figs. 7 and 8, it appears that the induced pressure field can have a significant effect on the nonequilibrium flow field along the first 10 ft of a highly cooled plate throughout the altitude range of 150-300 kft for flight Mach numbers in excess of 20. At lower flight speeds in this altitude range, however, the initial dissociation rate within the boundary layer even including the effect of the induced pressure field is so small that the boundary layer will

rema n completely frozen over plate lengths of practical interest unless $T_w/T_o > 0.25$.

In all cases where the induced pressure field has a significant effect on the nonequilibrium flow in the boundary layer, it is seen that most of this effect occurs in the strong interaction region. By the time the decaying induced pressure ratio, $p_e/p_\infty - 1$, drops to values of order unity or less (moderate to weak interaction regime), the difference between the solutions obtained by either including or neglecting the induced pressure field has already become comparatively small. This result justifies the use of Eq. (13) as a model of the pressure field in the present theory. The moderate-to-weak interaction regime tends to occur where the boundary layer has already relaxed appreciably away from the initial frozen state and would appear to be of interest mainly in connection with a nearly or completely equilibrated flow.

It should also be noted that the effect of the gas-phase recombination rate on each of the solutions presented here (except at the larger values of x for the adiabatic wall case shown in Fig. 6) was found to be completely negligible, as is illustrated, for example, in Fig. 5. This is not surprising, since, as previously pointed out, the dissociation rate is known to be the controlling reaction in a highly dissipative nonequilibrium boundary layer until the flow approaches very close to equilibrium.[3,4] As indicated in Figs. 5a through 8a, the boundary layer flows in the present examples (excepting the adiabatic wall case) are indeed far from equilibrium throughout, the maximum atom concentrations remaining well below their corresponding local equilibrium values up to values of $x = 10^4$. At the same time, the effects of the induced pressure field on the chemical behavior of the boundary layer of interest here become negligible well before the boundary layer approaches equilibrium, except when the wall temperature is extremely high.

## Significance of the Fully Viscous Region

According to the present strong interaction theory, the large self-induced pressures occurring near the leading edge of a flat plate in hypersonic flow can significantly enhance the dissociation rate and nonequilibrium atom concentration (and reduce the temperature) within the boundary layer for flight conditions of practical interest. However, in a number of the example cases illustrated in Figs. 5 through 8, the theory predicts that a good deal of the induced pressure field effect on relaxation takes place extremely close to the leading edge, where the strong interaction theory undoubtedly breaks down and there is instead a fully viscous flow region with no distinct inviscid layer. To more precisely define where the present analysis fails in this respect, one can use a rough estimate of the upstream limit of the strong interaction theory (downstream limit of the fully viscous theory) due to Oguchi.[16] Equating the pressure obtained from an analysis of the wedge-like fully viscous region for frozen flow to the pressure given by strong interaction theory, Oguchi finds that the latter theory should be (roughly) applicable beyond a certain distance $x_{down}$ given by

$$\bar{X}_{\infty_{down}} \approx \left(\frac{\bar{\gamma}_\infty - 1}{2P_{o,F}}\right) M_\infty^2 G \qquad (67)$$

where G is a function of the wall temperature ratio, $T_w/T_o$, alone (see Ref. 16) ranging from a value of 0.25 for a highly cooled wall to 0.80 for an adiabatic wall with $Pr = 1$ and a linear viscosity-temperature relation. Using Eq. (67), the values of $x_{down}$ appropriate to each of the numerical examples presented here have been computed and are indicated on Figs. 5a through 8a. Now, it can be seen from these figures that if one were to neglect the effect of the induced pressure field in computing the nonequilibrium boundary relaxation, significant departures from frozen flow would occur downstream of the fully viscous flow region near the leading edge. On this basis, the boundary layer theory would be acceptable for analyzing the nonequilibrium aspects of the flow problem and the more difficult, fully viscous region treated as a chemically frozen (perfect gas) problem. However, upon taking the effect of the induced pressure field into account according to strong interaction theory, it is seen instead that a considerable amount of the predicted nonequilibrium dissociation apparently takes place in the fully viscous flow region where the strong interaction theory breaks down. As expected, Figs. 5a through 8a show that an increasingly greater portion of the significant induced pressure field effect on chemical relaxation falls within this viscous region with increasing altitude, flight Mach number, and wall temperature.

On the basis of the foregoing estimates, it is clear that the strong interaction boundary layer theory overestimates the effect of the strong induced pressure field on the nonequilibrium boundary layer relaxation along a flat plate. This is because the induced pressure field involved increases without limit ($\sim x^{-1/2}$) as the leading edge is approached and thus gives too high a pressure (and dissociation rate) at sufficiently small values of x, whereas there actually occurs a leveling-off of the pressure to a certain plateau value as $x \to 0$ due to the wedge-like action of the fully-viscous region.[11,16,17] In this respect, the present theory serves as a useful upper limit in determining the effects of the induced pressure field on the nonequilibrium viscous flow along the plate. Moreover, since the induced pressure at the leading edge plateau can be quite large under the hypersonic, high-altitude flight conditions considered, there could still be a significant enhancement of the dissociation over the plate even when a more realistic model of the pressure field that includes the effect of the fully viscous flow region is used. If this indeed be the case, then the fully viscous region itself could contain nonequilibrium dissociation and would not be satisfactorily regarded as a chemically frozen flow.

## Summary and Conclusion

The effect of the self-induced pressure field on the nonequilibrium-dissociating hypersonic boundary layer flow along a sharp flat plate, using a strong interaction theory, has been studied. By neglecting the effect of recombination and employing the customary simplifying assumptions of $Pr = Le = 1$, constant mixture specific heat and a linear viscosity-temperature relationship, an analytical solution was obtained in the nearly frozen region near the plate leading edge. This solution completely describes all the effects of the induced pressure field on the nonequilibrium relaxation in the boundary layer, for either a completely catalytic or perfectly noncatalytic plate

surface, including the back effect of the growing dissociation level on the induced pressure field itself. Furthermore, an approximate solution was also obtained (including recombination) throughout the nonequilibrium relaxation region along the plate by means of an appropriate nonlinear, local extrapolation of the nearly frozen solution.

Numerical results of the theory were presented for a range of representative hypersonic free flight conditions and various wall temperatures. These examples indicated that the strong induced pressures encountered near the leading edge of a highly cooled plate can increase the degree of dissociation within the boundary layer over a 10 ft run of plate by a factor of three to four or more in the altitude range from 150-300 kft at flight Mach numbers above roughly 20. This effect is even more pronounced at higher wall temperatures but is relatively insensitive to the surface catalycity unless the wall temperature exceeds one quarter of the recovery temperature. Finally, it was found that the back effect of the growing dissociation level in the boundary layer on the displacement thickness reduces the local induced pressure below that computed for a frozen boundary layer, although this effect is relatively small (10-20 per cent) in the strong interaction region unless the wall temperature is very high.

Aside from the several simplifying assumptions employed in formulating the boundary layer equations and the usual limitations involved in using the hypersonic small disturbance theory in connection with the tangent wedge approximation for the inviscid flow, the present theory can be criticized in two respects. First, the relationship between the displacement thickness growth and induced pressure field employed, while accurate in the strong interaction region near the leading edge and correct in the limit of vanishing induced pressure, does not give a satisfactory account of the weak interaction region further downstream. Secondly, the method of nonlinear extrapolation whereby a local solution for the entire nonequilibrium region was obtained from the nearly frozen flow solution is not a satisfactory approximation all the way to equilibrium and should be checked by more accurate numerical solutions of the nonlinear partial differential equations governing the nonequilibrium boundary layer. Nevertheless, neither of these shortcomings (both of which can be improved) appear to bear significantly on the predicted effects of the induced pressure field. However, a far more serious limitation on the present work is the fact that a good deal of the significant enhancement of dissociation (and ionization) predicted apparently takes place in the fully viscous region close to the leading edge where strong interaction theory is no longer valid. Therefore, the present theory gives only an upper limit on the actual effects of the strong induced pressure field on the nonequilibrium viscous flow along the plate, so that a further study of the problem which takes into account the fully viscous region near the leading edge (and possible departures from frozen flow therein) seems warranted.

## Nomenclature

| | |
|---|---|
| $A$ | reaction rate parameter, Eqs. (5) and (6) |
| $C_\infty$ | Chapman-Rubesin constant |
| $\bar{c}_p$ | frozen specific heat of mixture |
| $D(a, T)$ | dissociation rate distribution function, Eqs. (2) and (5) |
| $F^*$ | function defined in Eq. (48) |
| $f$ | boundary layer stream function ($f' \equiv u/u_e$). |
| $G$ | parameter in fully viscous flow theory; see Eq. (67) |
| $g$ | $h_s/h_{s,e}$ |
| $H_\infty$ | $2a_\infty h_d/u_\infty^2$ |
| $h_d$ | specific dissociation energy of molecules |
| $h_s$ | total enthalpy, $\bar{c}_p T + ah_d + (u^2/2)$ |
| $I$ | displacement thickness function, Eq. (9) and (12) |
| $I_{c,1}, I_{c,2}$ | nonequilibrium flow displacement thickness integrals defined by Eqs. (55a), and (57b), respectively |
| $\mathcal{I}(\eta)$ | reaction rate integral defined by Eq. (47a) |
| $i(\eta)$ | $\mathcal{I}(\eta)/\mathcal{I}(\infty)$ |
| $K^*$ | $M_\infty(d\delta^*/dx)$ |
| $k_r'$ | recombination rate constant |
| $Le$ | Lewis number |
| $M_\infty$ | free stream Mach number |
| $n(x)$ | function defined by Eq. (11) |
| $Pr$ | Prandtl number |
| $P_I$ | induced pressure perturbation due to nonequilibrium dissociation, Eqs. (24) and (26b) |
| $p$ | static pressure |
| $p_{at}$ | standard atmospheric pressure |
| $p_{o,F}$ | constant in frozen boundary layer induced pressure field solution, Eq. (37) |
| $Q_w$ | $\sqrt{2/\xi_o}\,(2\dot{q}_w/u_\infty^2)$ |
| $\dot{q}_w$ | heat transfer rate per unit area |
| $R(a, T)$ | recombination rate distribution function, Eqs. (2) and (6) |
| $Re_{\infty,x}$ | $\rho_\infty u_\infty x/\mu_\infty$ (local Reynolds number based on free stream conditions) |
| $\mathcal{R}_m$ | molecular gas constant |

| | |
|---|---|
| $\mathcal{R}_u$ | universal gas constant |
| S | reaction rate parameter, Eqs. (5) and (6) |
| $s(\eta)$ | solution to Eq. (43) |
| $\bar{s}^*$ | parameter defined by Eq. (60) |
| T | absolute temperature |
| $T_d$ | dissociation temperature of molecules ($h_d/\mathcal{R}_m$) |
| $T_o$ | total temperature, $T_\infty + u_\infty^2/2\bar{c}_p$ |
| $T_{r,1}, T_{r,2}$ | reference temperatures in reaction rate, Eqs. (4)-(6). |
| u | velocity component parallel to free stream direction |
| $V_s(\eta)$ | $v_s(\eta)/v_s(\infty)$ |
| $v_s(\eta)$ | integral function defined by Eq. (46a) |
| x, y | coordinates parallel and normal to plate, respectively |
| $z(x)$ | function defined by Eq. (27) |
| a | atom mass fraction |
| $\beta^*$ | parameter defined by Eq. (49) |
| $\Gamma$ | characteristic (flow time/ dissociation time) parameter, Eq. (4) |
| $\Gamma_o$ | constant defined in Eq. (4) |
| $\bar{\gamma}$ | frozen specific heat ratio of mixture |
| $\delta^*$ | boundary layer displacement thickness |
| $\eta$ | similarity coordinate, Eq. (1) |
| $\eta^*$ | value of $\eta$ at boundary layer temperature maximum, Eq. (35) |
| $\mu$ | viscosity coefficient |
| $\xi$ | similarity coordinate, Eq. (1) |
| $\xi_o$ | $\rho_\infty \mu_\infty C_\infty u_\infty$ |
| $\rho$ | mixture density |
| $\sigma$ | local shock wave angle |
| $\phi(x)$ | function defined by Eq. (10) |
| $\bar{\chi}_\infty$ | $M_\infty^3 \sqrt{C_\infty} / \sqrt{Re_{\infty,x}}$, hypersonic viscous interaction parameter |
| $\omega$ | recombination rate temperature dependence exponent |

Subscripts

| | |
|---|---|
| cat | completely catalytic plate surface |
| down | downstream limit of fully viscous region (upstream limit of strong interaction theory) |
| EQ | equilibrium boundary layer flow |
| e | conditions at edge of boundary layer |
| F | chemically frozen boundary layer flow |
| I | first order, nearly frozen nonequilibrium perturbation |
| non-cat | perfectly noncatalytic plate surface |
| w | conditions on plate surface (wall) |
| $\infty$ | free stream conditions |

References


1. J.T.C. Liu, "On the Role of High Temperature Effects on Heat Transfer in Hypersonic Viscous Interaction," Developments in Mechanics, Plenum Press, New York (1961), Vol. 1 pp. 417-29.

2. W.M. Mann, Jr. and R.G. Bradley, Jr., "Hypersonic Viscid-Inviscid Interaction Solutions for Perfect-Gas and Equilibrium Real-Air Boundary Layer Flow," Advances in Astronautics, Plenum Press, New York (1963), Vol. 8 pp. 198-217.

3. W.E. Gibson, "Dissociation Scaling for Nonequilibrium Blunt-Nose Flows," ARS J. 32, 285-6 (1962).

4. W.J. Rae, "An Approximate Solution for the Nonequilibrium Boundary Layer Near the Leading Edge of a Flat Plate," I.A.S. Paper 62-178 presented at National Summer Meeting, June 1962.

5. L. Lees, "On the Boundary Layer Equations in Hypersonic Flow and Their Approximate Solution," J. Aeronaut. Sci. 20, 143-5, 1953.

6. L. Lees, "Laminar Heat Transfer Over Blunt-Nosed Bodies at Hypersonic Flight Speeds," Jet Propulsion 26, 259-69 (1956).

7. H.K. Cheng, J.G. Hall, T.C. Golian, and A. Hertzberg, "Boundary Layer Displacement and Leading Edge Bluntness Effects in High Temperature Hypersonic Flow," J. Aero/Space Sci. 28, 353-81 (1961).

8. F.K. Moore, "On Local Flat Plate Similarity in the Hypersonic Boundary Layer," J. Aero/Space Sci. 28 (10), 753-62 (1961).

W.D. Hayes and R.F. Probstein, Hypersonic Flow Theory, Academic Press Inc., New York (1959), p. 280.

C.F. Dewey, Jr., "Use of Local Similarity Concepts in Hypersonic Viscous Interaction Problems," AIAA J. 1 (1), 20-33 (1963).

H.T. Nagamatsu, H.A. Weil, and R.E. Sheer, Jr., "Heat Transfer to a Flat Plate in High Temperature Rarefied Ultra-High Mach Number Flow" ARS J. 32, 533-41 (1962).

P.M. Morse, and H. Feshbach, Methods of Theoretical Physics, McGraw-Hill Book Co., New York (1953), p. 440.

G.R. Inger, "Highly-Nonequilibrium Boundary Layer Flows of Multicomponent Dissociated Gas Mixture," ATN Series Report, Aerospace Corp., El Segundo, Calif.. (to be published).

14. G.R. Inger, "Nonequilibrium-Dissociated Stagnation Point Boundary Layers with Arbitrary Surface Catalycity," ATN-63(9206)-3, Aerospace Corp., El Segundo, Calif. (January 1963).

15. G.R. Inger, "Dissociated Laminar Boundary Layer Flows Over Surfaces with Arbitrary Continuous Distributions of Catalycity," ATN-63(9206)-2, Aerospace Corp., El Segundo, Calif. (November 1962).

16. H. Oguchi, "The Sharp Leading Edge Problem in Hypersonic Flow" Div. of Eng. Report ARL TN 60-133, Brown Univ. (1960).

17. H.T. Nagamatsu and R.E. Sheer, Jr., "Hypersonic Shock Wave-Boundary Layer Interaction and Leading Edge Slip," ARS J. 30 (5), 454-62 (1960).

TABLE I. TYPICAL VALUES OF DISPLACEMENT THICKNESS INTEGRALS FOR NONEQUILIBRIUM FLOW. OXYGEN, $\omega = -1.5$, $S = 0$

| $M_\infty$ | $T_w/T_o$ | $I_{c,1}$ | $I_{c,2}$ |
|---|---|---|---|
| 25 | 0.029 | 0.708 | 1.558 |
| 25 | 0.116 | 0.579 | 1.430 |
| 25 | 0.232 | 0.447 | 1.297 |
| 25 | 1.000* | 0.668 | 1.515 |
| 20 | 0.045 | 0.697 | 1.549 |
| 15 | 0.083 | 0.669 | 1.520 |

*NONCATALYTIC WALL

TABLE 2. VALUES OF PARAMETERS USED IN EXAMPLE CALCULATIONS

GAS: OXYGEN

$h_d = 1.649 \times 10^8$ FT$^2$/SEC$^2$

$T_d = 59{,}000°K$

$\omega = -1.5$

$S = 0$

$T_{r,1} = 4500°K$

$k_r^1 = 5 \times 10^{14}$ CM$^6$/MOLE$^2$-SEC

$\overline{c_p} = 9800$ FT$^2$/SEC$^2$ - °K

$\alpha_\infty = 0$

$C_\infty = 1$

$A = 16$

$\overline{\gamma_\infty} = 1.40$

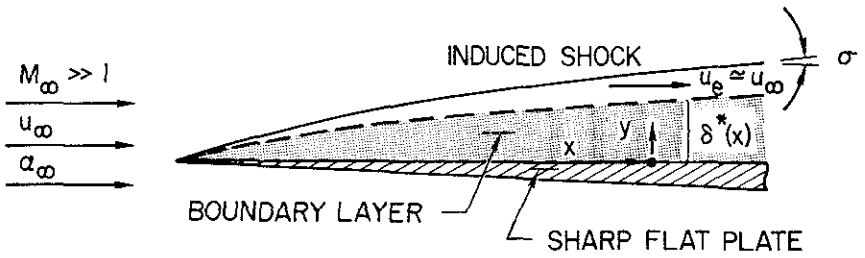


FIG. 1. FLOW CONFIGURATION

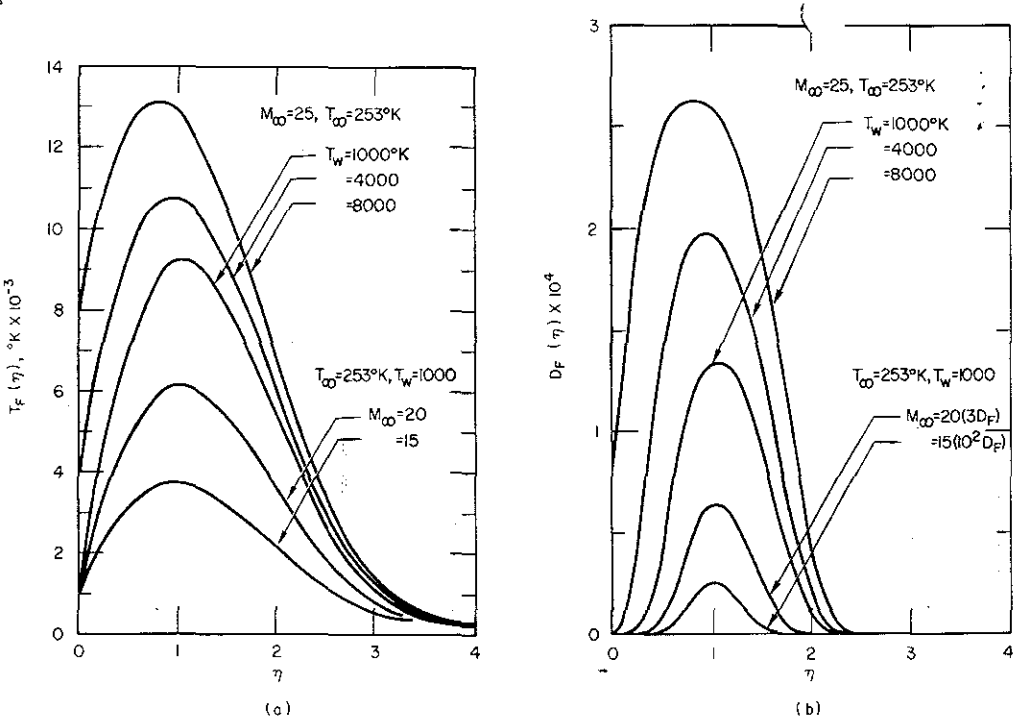


FIG. 2. TEMPERATURE AND DISSOCIATION RATE PROFILES ACROSS THE BOUNDARY LAYER AT PLATE LEADING EDGE

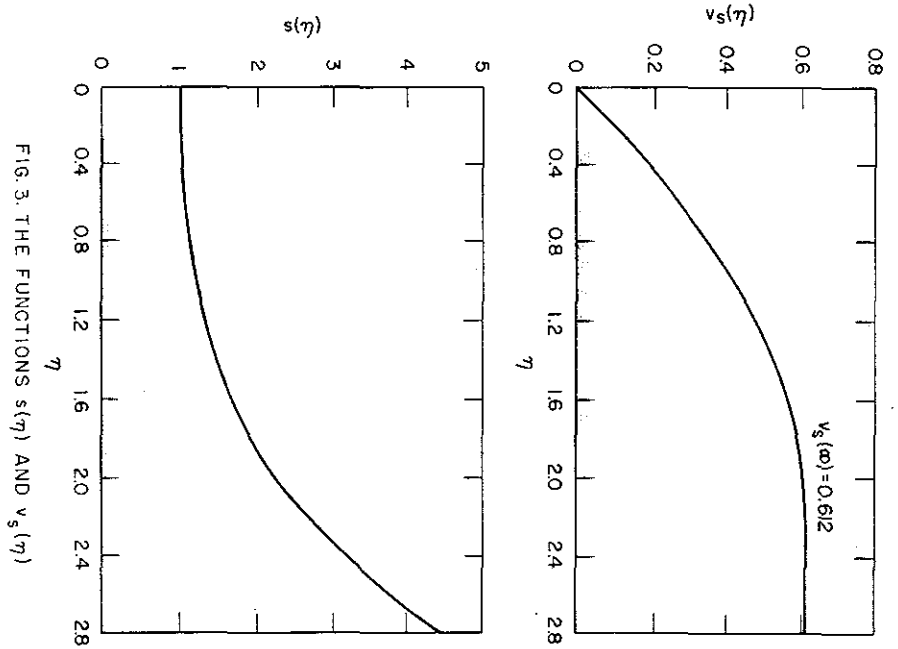


FIG. 3. THE FUNCTIONS $s(\eta)$ AND $v_s(\eta)$

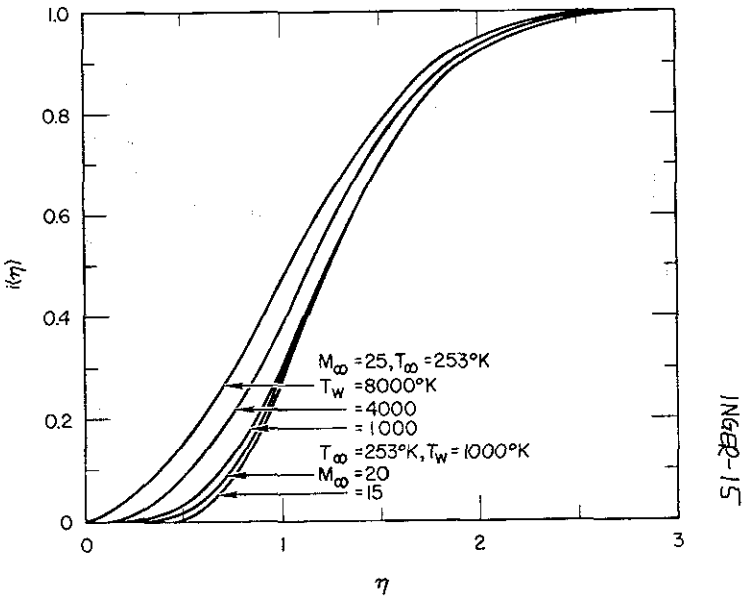


FIG. 4. NORMALIZED REACTION RATE INTEGRAL DISTRIBUTIONS ACROSS THE BOUNDARY LAYER

INGER-15

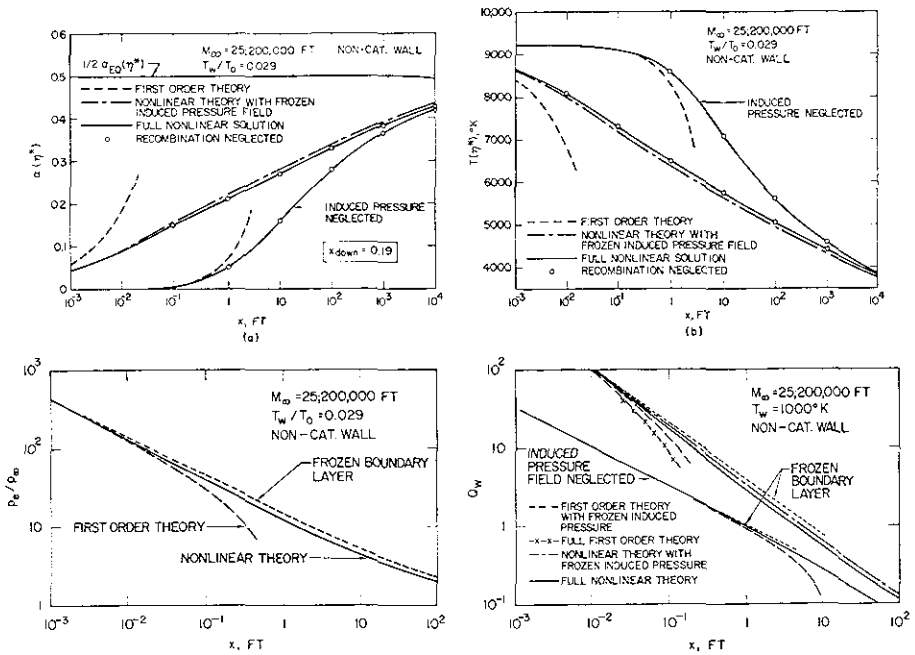


FIG. 5. DISTRIBUTIONS OF (a) MAXIMUM ATOM CONCENTRATION, (b) MAXIMUM TEMPERATURE, (c) INDUCED PRESSURE, AND (d) HEAT TRANSFER ALONG A HIGHLY COOLED NONCATALYTIC PLATE. $M_\infty$ = 25; 200,000 FEET ALTITUDE, $T_w/T_0$ = 0.029.

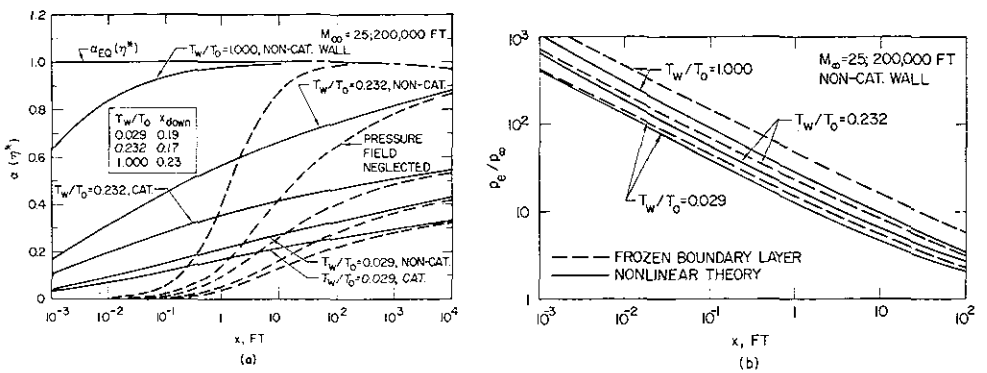


FIG. 6. EFFECT OF WALL TEMPERATURE AND SURFACE CATALYCITY ON (a) MAXIMUM ATOM CONCENTRATION AND (b) INDUCED PRESSURE FIELD. $M_\infty$ = 25; 200,000 FT ALTITUDE.

INGER-16

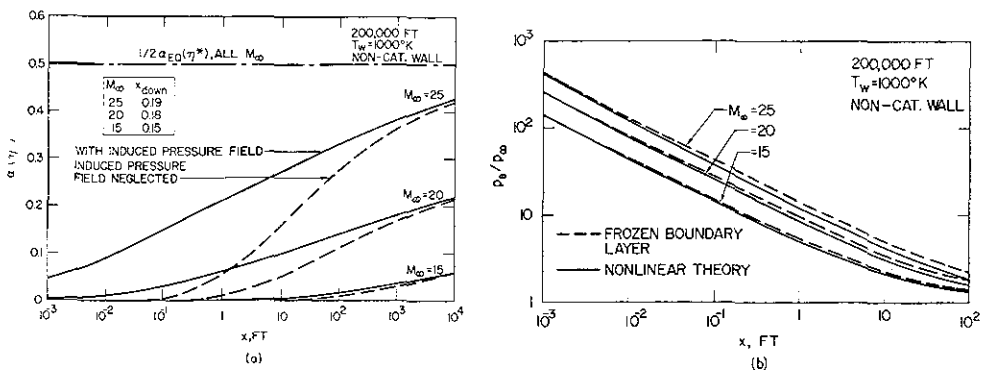


FIG. 7. EFFECT OF FREE STREAM MACH NUMBER ON (a) MAXIMUM ATOM CONCENTRATION AND (b) INDUCED PRESSURE FIELD. 200,000 FT ALTITUDE, $T_w$ = 1000°K

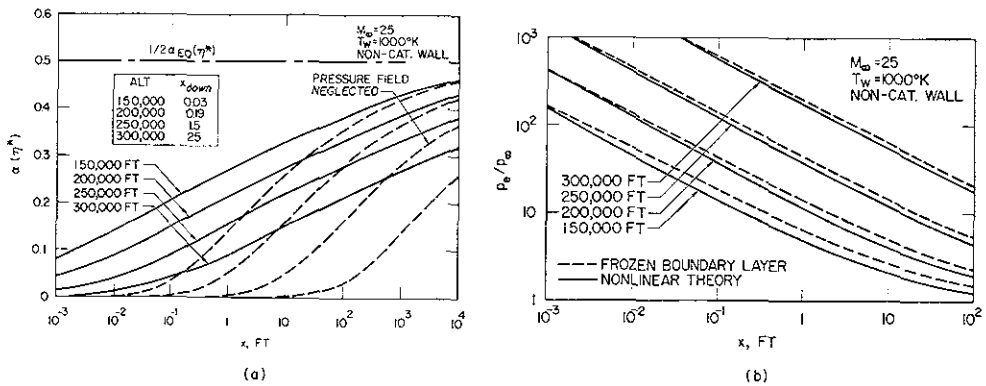


FIG. 8. EFFECT OF ALTITUDE ON (a) MAXIMUM ATOM CONCENTRATION AND (b) INDUCED PRESSURE FIELD. $M_\infty$ = 25; $T_w$ = 1000° K